COULD "FLAKES" OF NEUTRAL PARAMAGNETIC OR DIPOLAR MOLECULES EXPLAIN BEAM LOSSES IN THE LHC?*

G. Franchetti[1], GSI, Darmstadt, Germany
F. Zimmermann, CERN, Geneva, Switzerland
[1]also at HFHF, Frankfurt, Germany

Abstract

"Flakes" of neutral water or oxygen molecules carrying an electric or magnetic dipole moment can be attracted and trapped by the electromagnetic field of the circulating LHC proton beam. The possible presence of such flakes in the vacuum system could explain beam losses and beam instabilities encountered during the 2017 and 2018 LHC runs, and the observed effect of an external magnetic field.

INTRODUCTION

At large accelerator laboratories, such as GSI [1], CERN [2], or BNL [3], the vacuum pressure in the beam pipe of storage rings ranges from 10^{-8} to 10^{-10} Pa. In cryogenic rings [4], the vacuum pressure p may reach a level of 10^{-13} Pa or less, at a low temperature T. A low vacuum pressure ensures a low density of atoms and molecules, according to $n = p/(k_B T)$, with k_B the Boltzmann constant. The residual gas density n is a key quantity defining the "beam lifetime". In fact, the presence of neutral vacuum molecules in accelerator beam pipes lead to occasional collisions between beam particles and vacuum molecules, which may create several undesirable effects, ranging from the emission of beamstrahlung photons by beam electrons or positrons, over the stripping of electrons from partially stripped heavy-ion beam particles, to the fragmentation of the neutral molecule itself. The consequences of the beam-gas collisions may vary between a mild drop in the beam lifetime to a nearly catastrophic phenomenon, as in the case of a dynamical vacuum instability [5]. More generally, the presence of ionized gas molecules or liberated electrons inside the accelerator beam pipe can have undesired consequences, such as the creation of an electron cloud [6–10].

In this paper, we present a study of the dynamics of neutral molecules under the effect of the beam electromagnetic fields. We discuss a possible accumulation of neutral molecules in the vicinity of the beam [11], with potential negative impact on the beam lifetime. Then, inspired by observations in the LHC [12], we examine a possible mitigation by the installation of weak solenoid magnets.

NEUTRAL MOLECULE DYNAMICS

At first sight, neutral particles are not affected by an electromagnetic field unlike particles carrying an electric charge. However, the situation can be different for neutral molecules which may exhibit a non-homogeneous charge distribution.

To first order, this charge distribution $\rho(\vec{r})$ is characterized by its electric dipole moment $\vec{p} = \int \vec{r} \rho_M(\vec{r}) dv$. A similar discussion applies to the intrinsic magnetic field of a molecule, which may be characterized by a magnetic dipole moment $\vec{\mu}$.

In general, the geometry of a molecule is not rigid, but exhibits an equilibrium configuration of its elementary particles subject to internal restoring forces, which, for example, give rise to natural vibration states of the molecule around an equilibrium mechanical geometry. The frequency of these internal oscillations is high.

The effect of an homogeneous electric or magnetic field on a molecule with a dipole moment is to inflict a torque. If the field is not homogeneous a net force on the center of mass will also arise. These forces and torques are as follows [13]:

$$\begin{cases} \vec{\tau} = \vec{p} \times \vec{E} + \vec{\mu} \times \vec{B} \\ \vec{F}_{cm} = (\vec{p} \cdot \nabla)\vec{E} + (\vec{\mu} \cdot \nabla)\vec{B} \end{cases} . \tag{1}$$

The typical response of the molecule to a dipole-moment induced torque is an oscillation with frequency $\omega_E = \sqrt{pE/I_i}$, and $\omega_B = \sqrt{\mu B/I_i}$, where I_i denotes the moment of inertia of the molecule. The effect of the torque changes the orientation of the molecule according to its moment of inertia $I_i = ML^2$, with L a characteristic length of the molecule and M the molecule mass. The change of the molecule's orientation angle θ is

$$\frac{d^2\theta}{dt^2} = \omega_E^2 \hat{p} \times \hat{E}, \tag{2}$$

where $\hat{p}$ and $\hat{E}$ designate unit vectors in the direction of $\vec{v}$ and $\vec{E}$, respectively. The dynamics of the center of mass is instead governed by

$$\frac{d^2\vec{r}_{cm}}{dt^2} \propto \frac{pE}{M}(\hat{p} \cdot \nabla)\hat{E} = L^2 \omega_E^2 (\hat{p} \cdot \nabla)\hat{E}. \tag{3}$$

As L is small, oscillatory rotational motion of the molecule is much faster than the motion of its center of mass over a distance with a significant field change. Hence, we can approximately consider an effective dipole moment aligned with the respective field.

We next consider the electric and magnetic field generated by the beam in an accelerator.

EFFECT OF THE BEAM FIELD

For an axisymmetric coasting beam with a Gaussian particle distribution, the strength of the electric

MC5: Beam Dynamics and EM Fields

D02 Non-linear Single Particle Dynamics

and magnetic field is dependent only on the radial distance of a particle from the beam center according to $B(r), E(r) \propto \frac{I}{\sigma} \frac{\sigma}{r} \left[1 - \exp(-\frac{1}{2} \frac{r^2}{\sigma^2}) \right]$ with I the beam current, and σ the rms beam size. Note that in Eq. (1) the electromagnetic field enters in the dynamics through the "nabla" operator. Therefore, the effect on the center of mass is not the usual one created by space charge forces, but it is generated from a space derivative of a "dipole moment aligned with the local field". This creates an unusual force [11] sketched in Fig. 1. For the EDM case, the force disappears at a specific radius r_e, which depends only on the beam size and not on the beam current. The dynamics of EDM neutral molecules is complex. The timescale of the dynamics becomes more evident after rescaling the molecule position with the rms beam size as σ and rescaling the time to the unit $2\pi / \omega_E$. We find in Ref. [11] that the dynamics timescale of Eq. (3) is determined by the ratio L^2 / σ^2, which is extremely low for realistic parameters, hence the difficulty in simulating the dynamics.
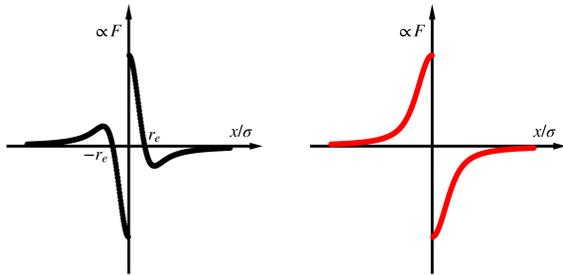

Figure 1: Forces exerted on the center of mass of a molecule, as a function of normalised transverse position. Note the substantial difference between EDM (black markers), and MDM (red markers), but also the difference with respect to usual space-charge forces expected from the beam fields.

The initial conditions for the motion of the neutral molecules is determined by the thermodynamics of the vacuum. At the starting point, we consider the molecules to be in thermodynamical equilibrium, or that there transverse rms velocity is $v_{rms} = \sqrt{k_B T / M}$. Note that the forces of Eq. (1), represented in Fig. 1, create a potential Well, which can effectively trap neutral molecules, provided they have a kinetic energy never large enough to escape. As the initial kinetic energy of a molecule can be related to an rms velocity, directly linked to the temperature, a characteristic trapping temperature can be associated with a specific strength of the force in Fig. 1. Clearly this temperature results from a combination of beam properties as beam current I, beam size σ, and the dipole moment strengths p and μ. Carrying out the mathematics one finds that the respective trapping temperatures T^* for EDM and MDM molecules are

$$T_p^* = \frac{1}{\pi \epsilon_0 k_B c} \frac{I}{\sigma} p, \qquad T_\mu^* = \frac{1}{\pi \epsilon_0 k_B c} \frac{I}{\sigma} \frac{\mu}{c},$$

as shown in [11]. If $T / T^* \gg 1$, we expect that neutral molecules are not trapped by the electromagnetic beam field.

If a significant portion of molecules is trapped, the oscillations of the molecules around equilibrium radius produce an enhanced density structure, evolving with time as is shown in Fig. 2: here the horizontal axis represent the time in units of linear oscillation periods around the equilibrium radius r_e. Note that this picture will change according to the ratio of the actual gas temperature T and T^*. The density enhancement increases for a smaller ratio of T/T^*. If heavy flakes are formed, e.g. each consisting of N molecules, their trapping temperature $T_f^* = NT^*$ is larger than the T^* of individual molecules, which, therefore, enhances the density increase, and could lead to some of the potential problems described in the Introduction.
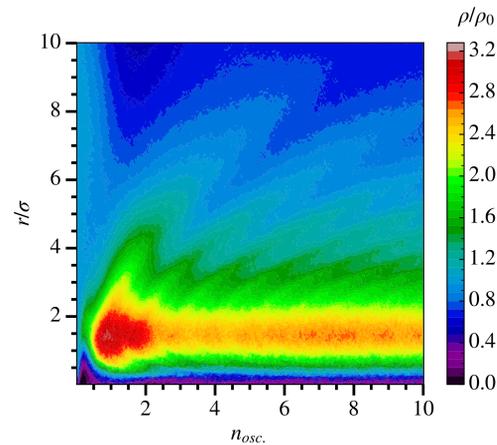

Figure 2: Radial density evolution for EDM molecules for $T/T_p^* = 0.05$.

MITIGATION BY SOLENOIDS

The alignment of the dipole moment to the correspondent field is influenced not only by the beam field, but by external fields as well. For example, the dynamics of MDM molecules will be affected by adding an external magnetic field, such as the one created by a solenoid. It is noteworthy that, in the LHC Run 2, the installation of a local 60 G solenoid at a particular, critical location "16L2", with a suspected surface layer of frozen air molecules, was effective in suppressing locally induced beam loss and instabilities [12].

The total magnetic field $\vec{B}$ is now the results of the sum of the beam and solenoid fields, and the MDM is considered aligned to $\vec{B}$. In this situation the potential Well will be changed, and hence T^*. The key parameter is the ratio of the maximum solenoidal field over the maximum beam field, $\chi = B_{s,\max} / B_{b,\max}$. Given a gas temperature T, and fixing the value of χ, we obtain a corresponding T^*: when $T/T^* > 1$ trapping will become difficult, and a beneficial disruption of the neutral molecule dynamics will result.

As an alternative to the procedure just sketched, we can estimate the impact of a solenoid also as follows. Through a direct integration of the magnetic field created by each tiny segment of the solenoid coils we compute the exact local solenoid field at the position of a molecule. We then apply Eq. (1) assuming that the dipole field is aligned with

MC5: Beam Dynamics and EM Fields

D02 Non-linear Single Particle Dynamics

the local solenoidal field. The result of this procedure is shown in Fig. 3, we call L_s the solenoid length, and R_s is the solenoid radius. The quantity F is a scaled force obtained by replacing the dipole moment by a unity vector and normalising the magnetic field to its maximum, namely $\vec{\mu} \to \hat{\mu}$, $\vec{B} \to \hat{B}$. The curves in Fig. 3 were computed at a radial position $r = 0.1R_s$ and $r = 0.9R_s$. From this picture the actual physical force can be obtained as $F = (\mu B_{max}/R_s)F$, with B_{max} the field at the solenoid center (transverse and longitudinal). The solenoid becomes effective in mitigating the beam induced dynamics when the force it generates is of the same order of magnitude as of the force induced by the beam electromagnetic field.
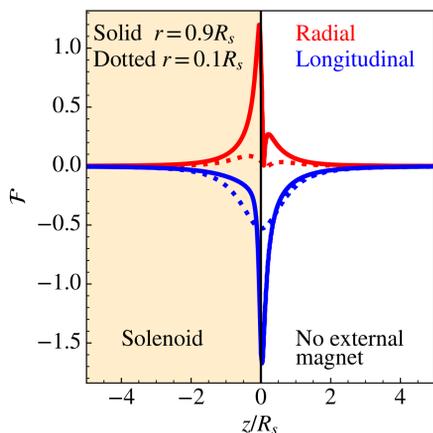

Figure 3: Normalised force at several longitudinal positions. The solenoid coil extends over negative z values and ends at $z = 0$. Shown in red is the resulting radial force, and in blue the longitudinal one. The radial position of the particle is at $r = 0.9R_s$ (solid) and $r = 0.1R_s$ (dotted). The results are relatively insensitive to L_s/R_s as long as $L_s/R_s > 10$.

According to the analysis of Ref. [11], the maximum value of the force exerted on a molecule due to the beam field is $F_{max} = k_B T^*_\mu/(4\sigma)$. Hence, a beneficial effect of the solenoid is expected if $(\mu B_{max}/R_s)F \geq k_B T^*_\mu/(4\sigma)$, namely for a maximum solenoidal field of

$$B_{max} \geq \frac{1}{4}\frac{R_s}{\sigma}\frac{k_B}{\mu}\frac{1}{F}T^*_\mu. \tag{4}$$

Figure 3 shows that the contribution of the solenoid is maximum at its end region, where the field gradient is the strongest (fringe field). Hence, as a first exploratory step we inspect when these regions of the solenoids may disrupt the molecular dynamics induced by the electromagnetic beam field. From Fig. 3 we deduce a reference value $F \simeq 0.5$ as a typical average value of the transverse and longitudinal normalized forces in the solenoid fringe-field region.

Considering a gas of MDM molecules like O_2 with $\mu = 2.8$ BM (units of Bohr magneton) and an LHC beam at injection energy with an average current of $I \approx 0.5$ A and $\sigma \approx 2$ mm, we find $T^*_\mu = 8$ mK. For a solenoid with $R_s/\sigma = 10$, Eq. (4) then yields $B_{max} \geq 30$ G, two times lower than the 60 G field successfully applied in the LHC.

We note that the required B_{max} increases, by about a factor of 7, as the LHC beam size shrinks during acceleration to top energy. However, in the above estimate we compared the force from the solenoid with the strongest possible effect of the beam. Most molecules participating in the build up originate in outer regions of the beam pipe, where the beam force is weaker, and where, hence, a weaker solenoid suffices to prevent their attraction by the beam field.

Interestingly, Eq. (4) holds even in the case of flake formation [11]. In fact, for an arbitrary clustering process involving N molecules, the flake trapping temperature is $T^*_{\mu,f} = NT^*_\mu$, and the magnetic dipole moment of the flake $\mu_f \approx N\mu$, so that $T^*_{\mu,f}/\mu_f = T^*_\mu/\mu$. In consequence, the impact of the solenoid on the density enhancement changes with the type of clustering. For a situation with no flakes, the trapping temperature is extremely low ($T^*_\mu = 8$ mK) compared with the LHC beamscreen temperature of $T \approx 5$ K. Hence, no enhancement of the density of molecules should be possible, even without solenoid, and the dynamics of single residual gas molecules is dominated by their thermal motion.

However, in case a flake formation happened, larger molecule aggregates have a larger trapping temperature, which would reduce T/T^*_μ, allowing, in the absence of a solenoid, the formation of regions of higher density through a pinch-like dynamics, as in Fig. 2 (see Ref. [11] for more details). Here, for heavy flakes, the solenoid has an important effect, especially in the vicinity of the solenoid edges.

Although we do not know the exact processes leading to flake formation at cryogenic temperature in the LHC and neither the size of such flakes, the properties of Eq. (4) reveal that the disruptive action of the solenoid remains the same, independently of the flake mass. This implies that the solenoid will prevent heavy flakes from constructing a coherent pinch-like dynamics, irrespective of their trapping temperature $T^*_{\mu,f}$. This property is remarkable: the solenoid allows solving a problem without exactly knowing how bad it is: once B complies with Eq. (4), the higher T^*_μ the more effective will be the solenoid in avoiding a density increase. At last, we have found an example of a *good* fringe field!

OUTLOOK

A first analysis was presented of the effect of a solenoid on the motion of neutral molecules with a magnetic dipole moment subject to the electromagnetic beam field. We have argued that if the solenoid field creates a force comparable of the one from the beam, the pinch mechanism is disrupted and regions of enhanced molecule density can no longer form in the vicinity of the beam. While, in the future, more detailed studies and simulations can be carried out, the results of this first study could already serve to motivate the application of weak solenoids in regions with suspected flake formation.

ACKNOWLEDGEMENTS

REFERENCES

[1] P. Spiller *et al.*, "The FAIR Heavy Ion Synchrotron SIS100", *Journal of Instrumentation*, vol. 15, no. 12, p. T12013, 2020. doi:10.1088/1748-0221/15/12/T12013

[2] V. Baglin, "Cryopumping and Vacuum Systems", in *Proc. CAS - CERN Accelerator School: Vacuum for Particle Accelerators*, Glumslöv, Sweden, Jun. 2017, pp. 1-34. arXiv:2006.01574

[3] U. Iriso and W. Fischer, "Electron induced molecular desorption from electron clouds at the Relativistic Heavy Ion Collider", *Physical Review Special Topics - Accelerators and Beams*, vol. 8, no. 11, p. 113201, Nov. 2005. doi:10.1103/physrevstab.8.113201

[4] R. von Hahn *et al.*, "The Cryogenic Storage Ring CSR", *Review of Scientific Instruments*, vol. 87, no. 6, p. 063115, 2016. doi:10.1063/1.4953888

[5] E. Mustafin, O. Boine-Frankenheim, I. Hofmann, H. Reich-Sprenger, and P. Spiller, "A theory of the beam loss-induced vacuum instability applied to the heavy-ion synchrotron SIS18", *Nuclear Instruments and Methods in Physics Research Section A: Accelerators, Spectrometers, Detectors and Associated Equipment*, vol. 510, no. 3, pp. 199–205, 2003. doi:10.1016/s0168-9002(03)01811-4

[6] K. Ohmi, "Beam and photoelectron interactions in positron storage rings", *Physical Review Letters*, vol. 75, no. 8, pp. 1526–1529, Aug. 1995. doi:10.1103/physrevlett.75.1526

[7] F. Zimmermann, "A simulation study of electron-cloud instability and beam-induced multipacting in the LHC", CERN, Geneva, Switzerland, Rep. LHC-Project-Report-95, Feb. 1997.

[8] O. Dominguez *et al.*, "First electron-cloud studies at the Large Hadron Collider", *Physical Review Special Topics – Accelerators and Beams*, vol. 16, no. 1, p. 011003, Jan. 2013. doi:10.1103/PhysRevSTAB.16.011003

[9] G. Rumolo *et al.*, "Electron Cloud Effects at the LHC and LHC Injectors", in *Proc. 8th Int. Particle Accelerator Conf. (IPAC'17)*, Copenhagen, Denmark, May 2017, pp. 30-36. doi:10.18429/JACoW-IPAC2017-MOZA1

[10] G. Iadarola *et al.*, "Progress in Mastering Electron Clouds at the Large Hadron Collider", presented at the 12th Int. Particle Accelerator Conf. (IPAC'21), Campinas, Brazil, May 2021, paper TUXA03, this conference.

[11] G. Franchetti, F. Zimmermann, and M. A. Rehman, "Trapping of neutral molecules by the beam electromagnetic field", *Physical Review Accelerators and Beams*, vol. 24, no. 5, p. 054001, May 2021. doi:10.1103/physrevaccelbeams.24.054001

[12] J. M. Jimenez *et al.*, "Observations, Analysis and Mitigation of Recurrent LHC Beam Dumps Caused by Fast Losses in Arc Half-Cell 16L2", in *Proc. 9th Int. Particle Accelerator Conf. (IPAC'18)*, Vancouver, Canada, Apr.-May 2018, pp. 228-231. doi:10.18429/JACoW-IPAC2018-MOPMF053

[13] E. Purcell and D. Morin, *Electricity and Magnetism*, Cambridge, UK: Cambridge University Press, 2013.